ELSEVIER

Contents lists available at ScienceDirect

# Materials Letters

journal homepage: www.elsevier.com/locate/matlet





# Characterization of crosslinked nanocellulose from oil palm frond fibers for enhanced drug-loaded hydrogels in antibacterial application

Y.L. Kong <sup>a,\*</sup> , M.Y. Leong <sup>b</sup>, M.Y. Harun <sup>c</sup>, W.F. Wong <sup>d</sup>, C.Y. Looi <sup>b,\*</sup>

- <sup>a</sup> Department of Engineering and Applied Sciences, American Degree Program, Taylor's University Lakeside Campus, 47500 Subang Jaya, Selangor Darul Ehsan, Malaysia
- b School of Biosciences, Faculty of Health and Medical Sciences, Taylor's University Lakeside Campus, 47500 Subang Jaya, Selangor Darul Ehsan, Malaysia
- c Department of Chemical and Environmental Engineering, Faculty of Engineering, Universiti Putra Malaysia, 43400 UPM Serdang, Selangor Darul Ehsan, Malaysia
- d Department of Medical Microbiology, Faculty of Medicine, Universiti Malaya, 50603 Kuala Lumpur, Malaysia

#### ARTICLE INFO

Keywords: Cellulose nanocrystals Antimicrobial efficacy Hydrogel Crosslinking

#### ABSTRACT

This study investigates the antibacterial efficacy and material properties of gelatin-based hydrogels incorporated with nanocellulose derived from oil palm frond fibers (CNC) and crosslinked with glutaraldehyde (GA) to optimize drug delivery systems. The hydrogels were loaded with either erythromycin (ERY) or tetracycline hydrochloride (TAC) and evaluated against *Pseudomonas aeruginosa*. Results demonstrated that the inclusion of GA significantly enhanced the antibacterial activity, particularly in TAC-loaded hydrogels, which achieved the largest inhibition zones. The study highlights the synergistic effect of CNC and GA in stabilizing hydrogel structures and improving drug release profiles, offering a promising approach for advanced antimicrobial applications in biomedical materials.

#### 1. Introduction

Oil palm frond (OPF) biomass, an underutilized plantation waste rich in cellulose (55.54 %), offers a promising source for cellulose nanocrystals (CNC) [1]. CNCs are obtained by removing amorphous cellulose from oil palm frond fiber (OPFF), yielding nanocrystals 5-70 nm wide and 100-300 nm long [2]. While their chemical composition can vary depending on extraction methods and raw material nature, they generally consist mostly of cellulose, with small amounts of lignin and hemicellulose. Recent studies report CNCs from OPFF containing 55.17 % cellulose, 14.67 % lignin, and 8.72 % hemicellulose [3]. Despite this, CNC from OPF has not yet been explored as a reinforcing agent in hydrogel systems. CNCs are non-toxic, biodegradable, and mechanically robust, ideal for enhancing antimicrobial agent efficacy [4]. Their nanoscale dimensions and surface functionality improve drug stability, loading, and antimicrobial performance [5,6]. Hydrogels, formed by crosslinked polymer chains, can be enhanced with CNCs to improve porosity, thermal stability, and drug release profiles [7]. While many hydrogel systems have demonstrated strong performance in specific applications, challenges such as poor mechanical integrity, uncontrolled swelling, and limited drug retention persist, particularly in systems using synthetic fillers. In contrast, this study employs a sustainable,

biocompatible CNC derived from underutilized OPFF, combined with glutaraldehyde (GA) crosslinking, to enhance hydrogel structure and antibacterial performance [8,9]. Surface morphology is analyzed using fractal theory to relate roughness and complexity to potential drug delivery behavior. This approach offers a promising and eco-friendly platform for developing improved hydrogel-based antimicrobial systems.

# 2. Materials and methodology

### 2.1. Extraction of CNC from OPFF and crosslinking process

CNCs were extracted from OPFF via drying, blending, sieving, chlorination, and sodium hydroxide treatment, followed by enzymatic hydrolysis (5 g/g). The CNCs were sonicated (20 kHz, 500 W, 15 mins), freeze-dried, and dispersed (0.5 g in 50 mL water). Gelatin (4.5 g) was added at 55  $^{\circ}\text{C}$  and crosslinked with 3 wt% glutaraldehyde. Erythromycin or tetracycline hydrochloride (0.1 wt%) was incorporated before gelation. Hydrogels were chilled, rinsed, UV-sterilized, and prepared in triplicate for testing.

E-mail addresses: kong.yeolee@taylors.edu.my (Y.L. Kong), chungyeng.looi@taylors.edu.my (C.Y. Looi).

<sup>\*</sup> Corresponding authors.

Y.L. Kong et al. Materials Letters 401 (2025) 139209

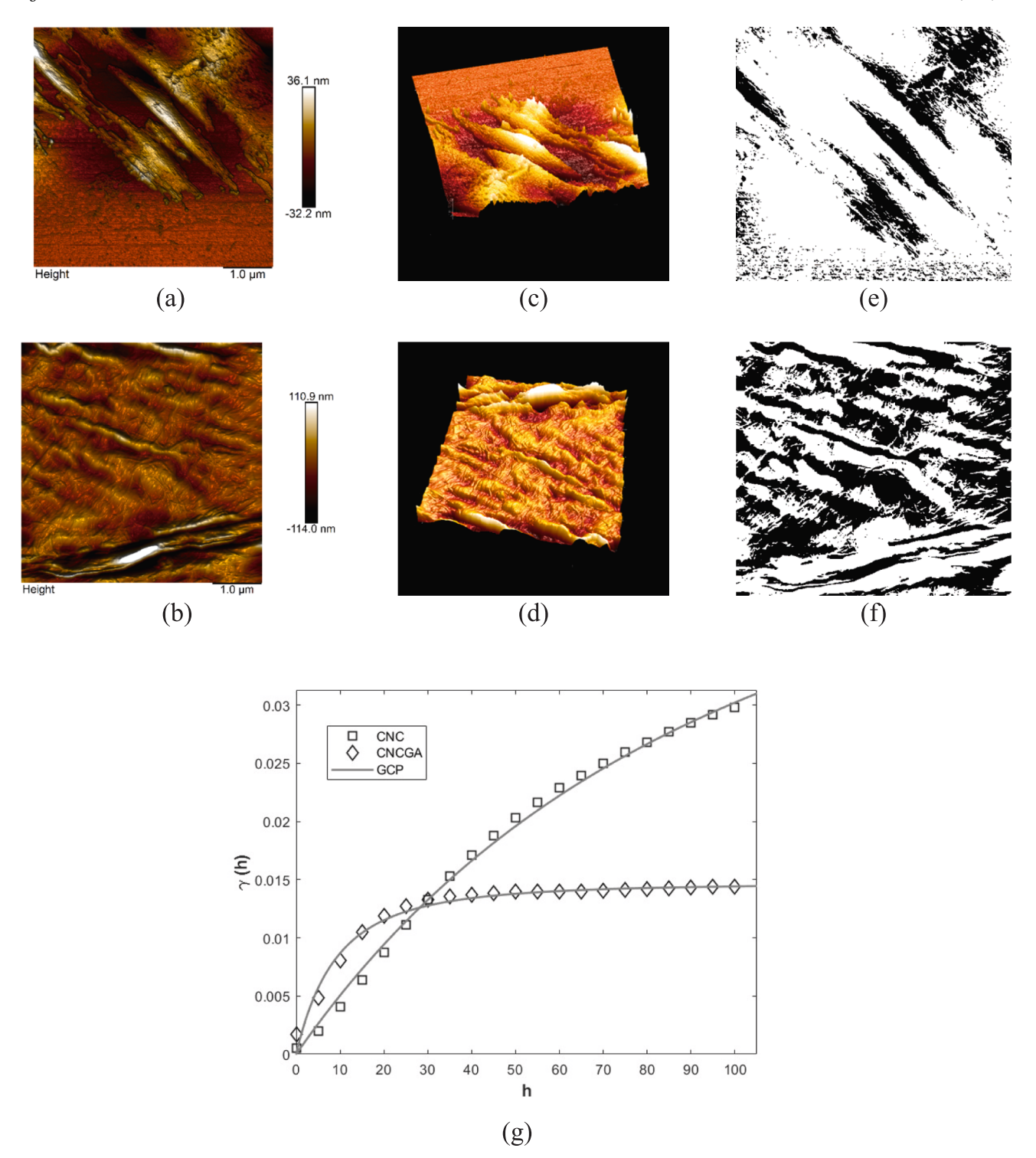


Fig. 1. AFM images and 3D surface topography of: (a, c) CNC without a crosslinker and (b, d) CNC crosslinked with glutaraldehyde. Threshold-processed images illustrate the distribution of (e) CNC alone and (f) crosslinked CNC. (g) Semivariograms generated using the generalized Cauchy process (GCP) model provide the fractal parameters.

# 2.2. Atomic Force Microscopy (AFM) characterization & image processing

Morphological changes before and after crosslinking were analyzed using AFM (Bruker Multimode 8, ScanAsyst) on enzymatically treated CNC (5 g/g) and CNC crosslinked with glutaraldehyde. The scans were performed at 5  $\mu m \times 5$   $\mu m$  with 512 sample lines and a scan rate of 0.9 Hz. The AFM images (Fig. 1) were processed and homogenized using the

generalized Cauchy process (GCP) to extract fractal parameters, with calculation details provided in our previous work [10]. The parameters  $\alpha$ ,  $\beta$ ,  $\alpha$ , and  $\sigma^2$  are fractal exponent, correlation length, scale parameter, and sample variance respectively:

$$\Gammaig(h;lpha,eta,a,\sigma^2ig)=(\sigma^2-rac{\sigma^2}{(1+|rac{h}{a}|^a)^{eta/lpha}}$$

**Table 1**Estimated morphological parameters of CNC and crosslinked CNC from the GCP model.

No.	Sample	а	$\sigma^2$	$\alpha$	β	Н	$D_f$	RMS (nm)
1	CNC	$102.53\pm0.44$	$0.07\pm0.00$	$\textbf{0.91} \pm \textbf{0.00}$	$0.81 \pm 0.00$	$0.60 \pm 0.00$	$\textbf{2.55} \pm \textbf{0.01}$	8.79
2	CNC/GA	$5.29 \pm 0.44$	$0.01\pm0.00$	$0.31 \pm 0.00$	$0.58 \pm 0.00$	$0.71\pm0.00$	$2.85 \pm 0.01$	25.80

 $(a = \text{spatial scale factor}, \sigma^2 = \text{sill variance}, \alpha = \text{fractal exponent}, \beta = \text{correlation exponent}, H = \text{Hurst exponent}, D_f = \text{fractal dimension}, RMS = \text{Root Mean Square}).$ 

**Table 2**Range of inhibition zones against *P. aeruginosa* within 48 hrs.

Hydrogel	Range of inhibition zones (mm)		
	Minimum	Maximum	
Gel/CNC/GA	-	-	
Gel/CNC/ERY	$14.6\pm0.0$	$17.6\pm0.1$	
Gel/CNC/GA/ERY	$15.9 \pm 0.4$	$26.7 \pm 0.3$	
Gel/CNC/TAC	$20.8 \pm 0.0$	$28.4 \pm 0.2$	
Gel/CNC/GA/TAC	$24.2 \pm 0.3$	$29.3 \pm 0.1$	

#### 2.3. Antimicrobial test and ANOVA

Sterile 5  $\times$  2 mm hydrogel discs were placed on Mueller-Hinton agar inoculated with bacteria, and inhibition zones were measured after 24 h incubation at 37 °C. Data were analyzed using two-way ANOVA in GraphPad Prism 10 to assess the effects of Formulation, Synthesis Method, and their interaction on inhibition zones, with results as mean  $\pm$  SD and significance at p < 0.05.

#### 3. Result and discussion

In hydrogels, fractal dimension helps relate surface roughness to bacterial interactions; higher values indicate greater complexity, which may enhance adhesion and antimicrobial effectiveness. As shown in Table 1 and Fig. 1g, the spatial scale factor (a) reflects the size of surface features, with larger a values indicating more spread-out structures and smaller a values denoting compact, tightly packed features. AFM images show that CNC without crosslinker (Fig. 1a, c, e) has a larger a, indicating a more diffuse topology, while CNC/GA (Fig. 1b, d, f) has a smaller a, reflecting denser features from crosslinking and a compact molecular structure [11]. The sill variance (a) measures surface height variability, with higher values indicating rougher textures. CNC without crosslinker shows greater variability and an irregular texture, whereas CNC/GA appears smoother and more uniform (Fig. 1b) due to enhanced molecular interactions and surface homogenization from crosslinking.

The fractal dimension  $(D_f)$  quantifies surface complexity, while the GCP model independently captures fractal scaling  $(D_f=3-\frac{\alpha}{2})$  and spatial connectivity through the correlation exponent  $(LRD=1-\frac{\beta}{2})$ . CNC shows greater connectivity with a broader structure, while CNC/GA has more isolated features, as seen in AFM images. CNC/GA's higher fractal dimension reflects fine details at smaller scales, with reduced connectivity and increased complexity defining its distinctive surface topology. The Hurst exponent (H) indicates that both CNC and CNC/GA have near-persistent surfaces, with CNC/GA showing smoother large-scale transitions. Its higher fractal dimension  $(D_f=2.85)$  reveals finer microscale complexity than CNC, and the GCP model offers a more comprehensive surface analysis than RMS alone [12].

Referring to Table 2, the addition of a GA crosslinker further enhanced antibacterial activity, likely by improving drug release or stabilizing the hydrogel structure. TAC-based hydrogels, particularly Gel/CNC/TAC/GA, showed stronger antibacterial effects, highlighting the synergistic benefits of combining CNC, GA, and TAC for enhanced inhibition zones and controlled drug release. The absence of inhibition zones in Gel/CNC/GA confirms that antibacterial effects stem from the active drugs, not the hydrogel matrix, with no increase in inhibition diameter observed after 24 h in any sample. Crosslinkers create a 3D

Table 3
Statistical significance of factors affecting inhibition zone diameters (two-way ANOVA).

Source	p-value	Significance
Formulation Synthesis Method Formulation × Synthesis Method	0.00002 0.947 0.997	Highly significant Not significant Not significant

polymer network that enhances mechanical strength, reduces solubility and swelling, limits flexibility, improves thermal stability, and modifies pore structure, affecting permeability and adsorption. Irregular crosslinker distribution raises  $D_f$  values, indicating greater structural complexity and improved hydrogel-antibiotic interactions [13]. Table 3 shows that the formulation had a highly significant effect on inhibition zone diameters (p = 0.00002), while the synthesis method and its interaction with formulation had no significant impact. Tetracycline-containing gels, especially Gel/CNC/TAC/GA, exhibited the strongest antibacterial activity, indicating enhanced efficacy with the addition of glutaraldehyde. Mechanical properties and drug loading capacity of this hydrogel system were reported in our previous study [10], while forthcoming work will address drug release behavior and its relation to fractal characteristics, diffusion, and bacterial adhesion [14].

#### 4. Conclusion

Crosslinking nanocellulose with glutaraldehyde (GA) significantly enhances the structural integrity, drug retention, and controlled release of gelatin-based hydrogels, leading to improved antibacterial performance. Higher fractal dimension  $(D_f)$  values in crosslinked samples highlight more complex surface structures that promote antibiotic interaction. This study introduces a novel approach by combining CNC derived from oil palm fronds with GA and antibiotics, demonstrating its potential as a sustainable and effective drug carrier system for biomedical applications. While the study focuses on *Pseudomonas aeruginosa* due to its pronounced response, additional tests against *Staphylococcus aureus* and CFU-based assays will be reported in future work.

# CRediT authorship contribution statement

Y.L. Kong: Writing – review & editing, Writing – original draft, Validation, Supervision, Methodology, Investigation, Funding acquisition, Formal analysis, Data curation, Conceptualization. M.Y. Leong: Formal analysis, Data curation, M.Y. Harun: Validation, Investigation, Formal analysis, Data curation, Conceptualization. W.F. Wong: Validation, Methodology, Formal analysis. C.Y. Looi: Writing – review & editing, Validation, Supervision, Formal analysis, Data curation, Conceptualization.

## **Declaration of competing interest**

The authors declare that they have no known competing financial interests or personal relationships that could have appeared to influence the work reported in this paper.

#### Acknowledgments

The authors thank the Malaysian Ministry of Higher Education (MOHE) for funding through Fundamental Research Grant Scheme (FRGS/1/2021/SKK06/TAYLOR/02/2).

#### Data availability

Data will be made available on request.

#### References

- [1] A. W. T. Owolabi, G. Arniza, W. Wan Daud, and A. F. M. Alkharkhi, "Effect of Alkaline peroxide pre-treatment on microfibrillated cellulose from oil palm fronds rachis amenable for pulp and paper and bio-composite Production," Bioresources, vol. 11, no. 2, Feb. 2016, doi: 10.15376/biores.11.2.3013-3026.
- [2] L.H. Zaini, et al., Effect of ammonium persulfate concentration on characteristics of cellulose nanocrystals from oil palm frond, J. Korean Wood Sci. Technol. 47 (5) (Sep. 2019) 597–606, https://doi.org/10.5658/WOOD.2019.47.5.597.
- [3] R. Randis, D.B. Darmadi, F. Gapsari, A.A. Sonief, Isolation and characterization of microcrystalline cellulose from oil palm fronds biomass using consecutive chemical treatments, Case Stud. Chem. Environ. Eng. 9 (Jun. 2024) 100616, https://doi.org/ 10.1016/j.cscee.2024.100616.
- [4] M.Y. Leong, Y.L. Kong, K. Burgess, W.F. Wong, G. Sethi, C.Y. Looi, Recent development of nanomaterials for transdermal drug delivery, Biomedicines 11 (4) (2023) 1–29, https://doi.org/10.3390/biomedicines11041124.
- [5] A. Gupta, S. Mumtaz, C.-H. Li, I. Hussain, V.M. Rotello, Combatting antibioticresistant bacteria using nanomaterials, Chem. Soc. Rev. 48 (2) (2019) 415–427, https://doi.org/10.1039/C7CS00748E.

- [6] A. Hosseinzadeh, A. Bozorg, P.R. Ranjbar, Magnetic graphene oxide functionalized with crystalline nanocellulose and zwitterionic polymers to achieve UF nanocomposite membranes of advanced performance, J. Environ. Chem. Eng. 11 (1) (Feb. 2023) 109198, https://doi.org/10.1016/j.jece.2022.109198.
- [7] S. Liu, S.A. Qamar, M. Qamar, K. Basharat, M. Bilal, Engineered nanocellulose-based hydrogels for smart drug delivery applications, Int. J. Biol. Macromol. 181 (2021) 275–290, https://doi.org/10.1016/j.ijbiomac.2021.03.147.
- [8] F. Wang, J. Li, G.C. Chen, H. Qi, K. Huang, S. Hu, Preparation and synergistic chemo-photothermal therapy of redox-responsive carboxymethyl cellulose/ chitosan complex nanoparticles, Carbohydr. Polym. (2021) 118714, https://doi. org/10.1016/j.carbpol.2021.118714.
- [9] S. Guleria, L. Chopra, Manikanika, Temperature responsive hydrogels for biomedical applications, Mater. Today Proc. 92 (2023) 356–363, https://doi.org/ 10.1016/j.matpr.2023.05.167.
- [10] Y. L. Kong, M. Y. Harun, M. Y. Leong, C. Y. Looi, and W. F. Wong, "Interpretation of morphological descriptors on nanocellulose from oil palm frond fibers under weak acid, strong acid, and enzymatic treatments," Mater Today Commun, vol. 37, no. November, 2023, doi: 10.1016/j.mtcomm.2023.107478.
- [11] J.E. Lee, S.W. Heo, C.H. Kim, S.J. Park, S.H. Park, T.H. Kim, In-situ ionic crosslinking of 3D bioprinted cell-hydrogel constructs for mechanical reinforcement and improved cell growth, Biomater. Adv. 147 (January) (2023) 213322, https://doi.org/10.1016/j.bioadv.2023.213322.
- [12] Y.L. Kong, S.V. Muniandy, M.S. Fakir, K. Sulaiman, Morphological image Interpretation of Organic phthalocyanine tetrasulfonic acid tetrasodium (TsNiPc) Film using Fractal Analysis, Appl. Surf. Sci. 301 (2014) 363–368, https://doi.org/ 10.1016/j.apsusc.2014.02.081.
- [13] L. Hossain, et al., Structure and swelling of cross-linked nanocellulose foams, J. Colloid Interface Sci. 568 (2020) 234–244, https://doi.org/10.1016/j. icis 2020 02 048
- [14] X. Xu, J. Sun, L. Bing, X. Cui, B. Jia, S. Bai, Fractal features of dual temperature/pH-sensitive poly(N-isopropylacrylamide-co-acrylic acid) hydrogels and resultant effects on the controlled drug delivery performances, Eur. Poly. J. 171 (May 2022), https://doi.org/10.1016/j.eurpolymj.2022.111203.